Molecular Ordering and Structure of Quasi-spherical Solutes by Liquid Crystal NMR and Monte Carlo Simulations: The Case of Norbornadiene

C. Aroulanda,[†,‡] G. Celebre,*[,†] G. De Luca,[†] and M. Longeri[†]

LXNMR SCAn group, Dipartimento di Chimica, Università della Calabria, 87036 Arcavacata di Rende, Rende (Cs), Italy, and Méthodologie RMN, UMR CNRS-UHP 7565, Université Henri Poincaré, BP 239, 54506 Vandoeuvre-lès-Nancy cedex, France

Received: March 3, 2006; In Final Form: April 5, 2006

Norbornadiene (a C_{2v} symmetry bicyclic rigid hydrocarbon) dissolved in three different nematic mesophases has been studied by liquid crystal NMR, to contribute to a better understanding of the influence of solvents on the solute's ordering and structure. The main results achieved by this work can be summarized as follows: (i) the order parameters obtained by the analysis of the ^{1}H NMR spectra (at different temperatures) were successfully reproduced by a recently proposed model of solute/liquid crystal interactions, by using Monte Carlo numerical simulations; (ii) the theoretical (B3LYP/6-31++G**) "equilibrium" geometry of norbornadiene, vibrationally corrected by using the force field calculated at the same level, is compatible (within, at most, a 5% error) with experimental LXNMR data. This leads to the conclusion that the structure is not significantly distorted by the tested solvents.

1. Introduction

Unlike solutes in "conventional" isotropic (fully disordered) liquids, probe molecules dissolved in uniaxial mesophases exhibit a "residual" statistical orientational order, responsible for the non-zeroing of anisotropic NMR observables,[1,2] namely, chemical shift anisotropy, indirect spin−spin coupling anisotropy, dipolar coupling, and quadrupolar splitting (this latter only when spin > 1/2 nuclei are present). All these quantities share information about the probe's ordering, and each of them contains peculiar pieces of information regarding different aspects of the nature of the solute (such as structure or charge density distributions). The choice of the suitable NMR observable to study the solute's ordering (possibly together with some other molecular property) entails of course pros and cons (e.g., about experimental feasibility, theoretical difficulties, accuracy of calculated order parameters, etc.): in this work, for example, the ^{1}H liquid crystal NMR spectroscopy (shortly, ^{1}H-LXNMR) has been chosen to treat the peculiar case of norbornadiene (Figure 1), a C_{2v} symmetry rigid hydrocarbon henceforth called NBD

Our choice of using ^{1}H-LXNMR (the "realm" of partially averaged dipolar couplings D_{ij}) has been motivated by the following two reasons. The first is that, besides the orientational dependence, only constants and geometrical factors are involved in the D_{ij} values expression (see formulas in the following). This fact is attractive because: (i) it allows us to acquire direct information about the structure of the solute in fluid condensed (liquidlike) phases and ^{1}H-LXNMR represents one of the few techniques (probably the only one) able to do that; (ii) no hypotheses and/or quite complicated calculations on electron density distributions (as, e.g., in the case of quadrupolar splittings or chemical shifts anisotropies and scalar coupling anisotropies) are required. The second reason to choose ^{1}H-LXNMR is that the high proton sensitivity ensures straightforward and rapid recordings of high-resolution NMR spectra in strongly orientating LXs (typical $D_{\infty h}$-phase-symmetry liquid-crystalline solvents as thermotropic nematics induce ordering in the solutes about 100/1000 times higher than lyotropics or assimilated nematics); so, the phenomenon of orientational order is emphasized and this allows us to work even with "quasi-spherical" shaped solutes, such as NBD (see modeling in the next sections). Besides these positive features, there are also limiting aspects of the ^{1}H-LXNMR technique, with the main being probably represented by the often difficult spectral analysis leading to the determination of the set of independent dipolar couplings (see the Spectral Analysis section). Since the complexity of the spectrum increases very quickly with the number of interacting spins, this inevitably limits the use of the technique to quite small molecules, where the number of spins does not exceed 12/14 (to give a size reference, "small" should be understood as the typical size of microwave spectroscopy (MW) treatable systems).

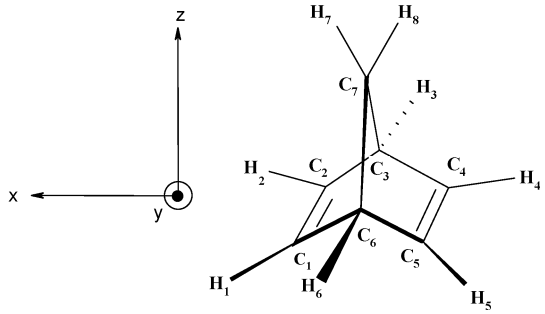

Figure 1. Structure of the C_{2v} symmetry norbornadiene (NBD), numbering of atoms, and definition of molecular frame (coinciding with the principal axis system (PAS) for the order parameter matrix, see text). H_1, H_2, H_4, and H_5 lie on the *xy*-plane, and the *z*-axis bisects the $H_7C_7H_8$ angle.

* To whom correspondence should be addressed. E-mail: giorgio.celebre@unical.it Fax: (39)0984493301. Tel: (39)0984493321.
† Università della Calabria.
‡ Univeristé Henri Poincaré.

10.1021/jp061345s CCC: $33.50
Published on Web 05/10/2006

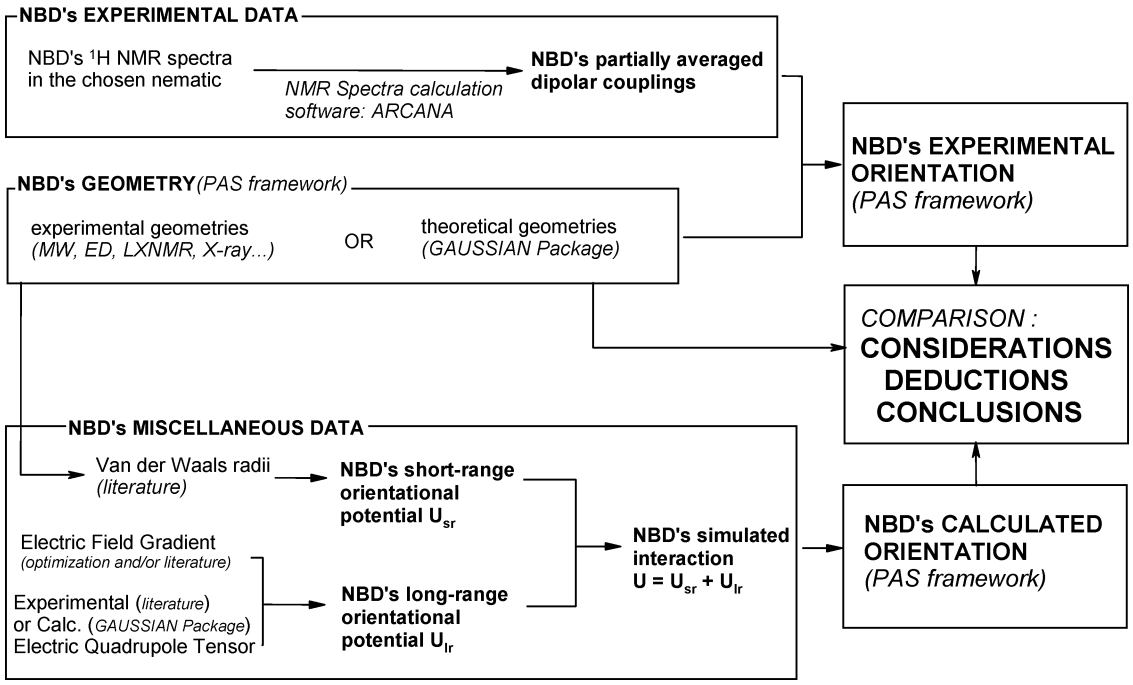

Figure 2. Analytical strategy proposed (MW, microwave; ED, electron diffraction; ARCANA and GAUSSIAN are software packages; see text for more details).

TABLE 1: Compositions of Liquid-crystalline NMR Samples

sample	mass of NBD (mg)[a]	solvent	mass of solvent (mg)[a]	% of NBD by weight	nematic−isotropic transition temperature T_{NI} (K)[b]
1	11.3	EBBA	376.8	2.9	339.2
2	8.2	MM	382.4	2.1	334.5
3	8.9	ZLI 1132	358.2	2.4	343.3

[a] The accuracy on weights is ±0.5 mg. [b] Temperatures at the transition point were determined by NMR. The accuracy of these determinations is ±0.1 K.

The structure of the present work is synoptically summarized in the flowchart of Figure 2: the geometry and order parameters of NBD at different temperatures were determined experimentally, then the ordering has been compared with that calculated using a Monte Carlo (MC) numerical simulation. Finally, conclusions are drawn about structural and orientational results.

2. NMR Experiments

The thermotropic LXs used as solvents in the present work are EBBA (i.e., *N*-(4′-ethoxybenzilidene)-4-*n*-butylaniline), ZLI 1132 (i.e., a mixture of three different *trans*-4-alkyl-(4-cyanophenyl)cyclohexanes and of *trans*-4-*n*-pentyl-(4′-cyanobiphenyl-4)cyclohexane), and the "Magic Mixture" (MM = 45 wt % EBBA + 55 wt % ZLI 1132). ZLI-type and EBBA are commonly used nematic solvents[1,2] giving high-resolution proton NMR spectra of small dissolved probes.[3] Furthermore, their use is of particular interest because of their weighted mixture MM. Indeed, it has been experimentally shown for H_2 (and inferred for larger medium-sized solutes, within a 10% error[4]) that the electric field gradient (EFG) felt by small-to-medium sized solutes in the MM around 300 K is near to zero,[4] thus minimizing the role of the long-range orientational contribution (see the Theoretical section). Therefore, when working in this medium, we may hope to decouple short- from long-range effects in the ordering of the solute. NBD was purchased from Aldrich, the liquid-crystalline phase ZLI 1132 from Merck Ltd−Darmstadt whereas EBBA was synthesized by using a procedure described elsewhere[5] (all of the chemicals were used without further purification). They were directly weighted into outside diameter (o.d.) 5 mm NMR tubes, and the NMR samples were sealed to avoid any variation in their compositions (Table 1). The NMR experiments were performed on a Bruker DRX 400 MHz (9.4 T) high-resolution spectrometer, equipped with a 5 mm broad band inverse probe and a BVT-3000 temperature control unit (accuracy, ±0.1 K).

After the temperature calibration process (performed before recording each series of spectra), the samples were heated to their nematic−isotropic transition temperature (T_{NI}) and shaken strongly to homogenize the nematic solution; then, they were left overnight in the magnetic field to improve the initial homogeneity. The spectra were recorded within 30−45 min intervals of thermostatisation for each temperature, with the T values being chosen to compare NBD dissolved in the various LXs in a common range of reduced temperature $T_{red} = T/T_{NI}$ (0.91−0.98 in EBBA and MM, 0.90−0.97 in ZLI 1132). The spectra (spectral resolution, ∼0.5 Hz/point) were recorded by increasing as well as decreasing temperatures and satisfactorily compared at each temperature; Gaussian apodization was then applied to enhance the apparent digital resolution.

3. Spectral Analysis

Beside chemical shifts differences and scalar couplings, the spectral analysis of the ^{1}H-LXNMR spectrum of a sample oriented by the spectrometer magnetic field $\mathbf{B}_0$ (fixing the *Z*-lab direction) yields the partially averaged spectroscopic ob-

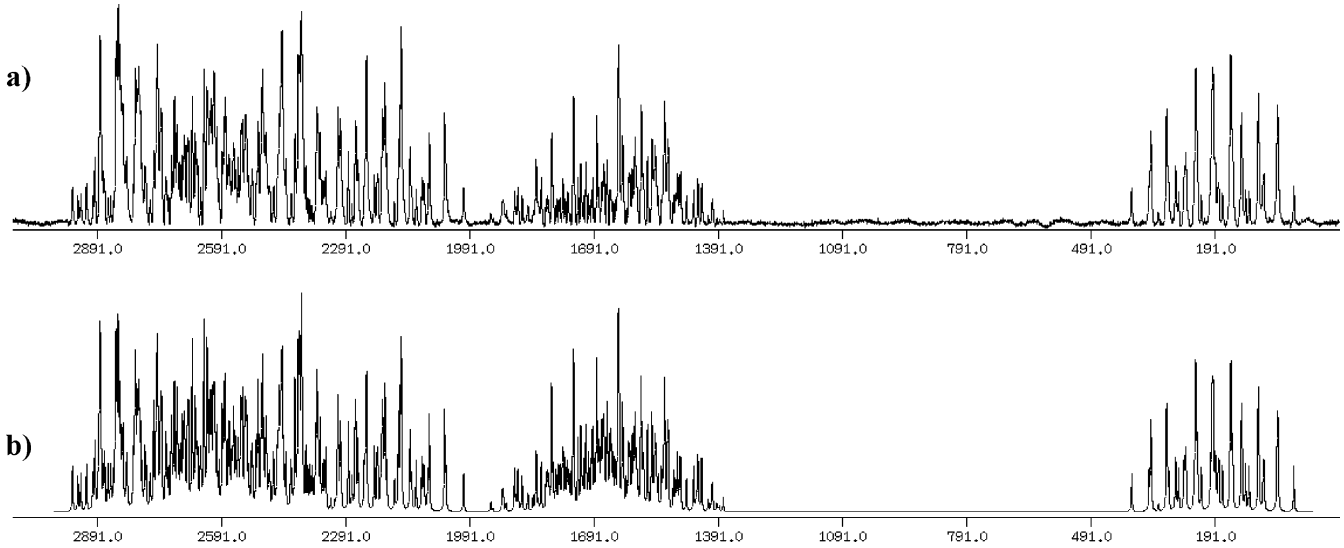

Figure 3. Proton NMR spectra of NBD dissolved in EBBA at 305 K (a) experimental and (b) calculated. See Table 1 for the exact sample composition.

TABLE 2: Chemical Shift Differences and Observed Residual Dipolar Couplings D_{ij}^{obs} (Hz) of NBD in the Liquid-crystalline Phase EBBA[a] (sample 1)

T (K) T_{red}	308.7 0.91	312.1 0.92	315.4 0.93	318.8 0.94	322.2 0.95	325.6 0.96	329.0 0.97	332.4 0.98
$\delta_1-\delta_3$	1281.046	1280.922	1281.33	1281.443	1281.792	1282.328	1282.658	1283.173
	± 0.110	± 0.073	± 0.080	± 0.073	± 0.075	± 0.088	± 0.095	± 0.148
$\delta_3-\delta_7$	613.558	613.121	612.397	611.817	610.925	609.919	609.041	608.252
	± 0.120	± 0.085	± 0.073	± 0.077	± 0.083	± 0.101	± 0.093	± 0.132
D_{12}	62.103	59.346	56.778	53.792	50.630	47.190	43.244	39.192
	±0.041	±0.027	±0.028	±0.027	±0.026	±0.029	±0.032	±0.077
D_{13}	5.552	5.174	4.962	4.636	4.331	4.031	3.676	3.273
	± 0.032	± 0.024	± 0.023	± 0.022	± 0.024	± 0.03	± 0.03	± 0.045
D_{14}	−20.217	−19.641	−18.922	−18.293	−17.421	−16.362	−15.295	−14.105
	± 0.047	± 0.033	± 0.033	± 0.034	± 0.033	± 0.032	± 0.041	± 0.085
D_{15}	−65.89	−63.744	−61.301	−58.88	−55.995	−52.808	−49.068	−42.957
	± 0.037	± 0.026	± 0.027	± 0.030	± 0.033	± 0.027	± 0.036	± 0.083
D_{16}	−48.816	−47.006	−45.104	−43.15	−40.948	−38.491	−35.569	−31.83
	± 0.035	± 0.022	± 0.025	± 0.023	± 0.026	± 0.032	± 0.038	± 0.044
D_{17}[b]	42.953	41.635	40.324	38.839	37.112	35.167	32.831	29.433
	± 0.103	± 0.015	± 0.017	± 0.013	± 0.012	± 0.015	± 0.016	± 0.024
D_{18}[b]	−2.896	−2.811	−2.662	−2.533	−2.357	−2.15	−1.997	−1.49
	± 0.102	± 0.015	± 0.017	± 0.013	± 0.012	± 0.015	± 0.016	± 0.024
D_{36}	15.626	14.988	14.342	13.565	12.831	11.964	11.033	9.771
	± 0.047	± 0.032	± 0.028	± 0.029	± 0.033	± 0.042	± 0.043	± 0.054
D_{37}	48.933	47.069	45.158	43.137	40.814	38.231	35.407	31.483
	± 0.026	± 0.02	± 0.017	± 0.017	± 0.02	± 0.025	± 0.025	± 0.031
D_{78}	−616.019	−594.964	−573.72	−550.445	−523.796	−494.127	−459.238	−412.647
	± 0.053	± 0.036	± 0.036	± 0.034	± 0.039	± 0.047	± 0.050	± 0.075
rms	0.3	0.3	0.3	0.2	0.3	0.3	0.3	0.4

[a] See Figure 1 for the numbering. [b] In the spectral analysis, the strongly correlated values of D_{17} and D_{18} were constrained together. Only for the lower value of temperature was it possible to relax them during the very last iteration cycles (see text for explanations).

servable $\tilde{T}_{ijZZ} \equiv D_{ij}^{obs} + (1/2)J_{ij}^{aniso}$. Anyway, when (as in our experiments) only proton−proton couplings are available, the J_{ij}^{aniso} term, usually quite small compared with D_{ij}^{obs}, is commonly neglected,[6] so as to approximate $\tilde{T}_{ijZZ} \approx D_{ij}^{obs}$. The determination of the set of independent dipolar couplings depends of course on the success of the analysis, the so-called "interpretation", of the LXNMR spectra. Given their intrinsic nature of "non-first-order" spectra (large magnitude of the couplings compared with the chemical shifts differences), the success of the interpretation is not a priori assured: it requires iterative and interactive calculations, in particular when the number of independent dipolar couplings increases. In the case of NBD, the analysis of the AA′A″A‴BB′CC′ eight-spin ^{1}H NMR spectra was carried out with the aid of a computer program called ARCANA[7] (no iterations on scalar couplings values have been performed; they have been used as given elsewhere[8]). As an example, an experimental spectrum of NDB in EBBA and its calculated counterpart are presented in Figure 3: we succeeded in determining all D_{ij} couplings of the NBD in that solvent at that temperature and finally its ordering in those conditions (assuming, of course, a geometry for the solute; see the next sections for details). Similar work has been done at different temperatures, for each of the three used nematic solvents. The obtained dipolar couplings and chemical shifts differences are reported in Tables 2−4 (since the D_{17} and D_{18} results strongly correlated, they were "constrained" together during the iterative process; then, typically at the lower T values, the constraint was relaxed in the final cycles of iterations, when nearly all the lines had already been assigned). In Tables 2−4, the root-mean-squared differences between experimental and

TABLE 3: Chemical Shifts Differences and Observed Residual Dipolar Couplings D_{ij}^{obs} (Hz) of NBD in the Liquid-crystalline Phase MM[a] (sample 2)

T (K) T_{red}	304.4 0.91	307.7 0.92	311.1 0.93	314.4 0.94	317.8 0.95	321.1 0.96	324.5 0.97	327.8 0.98
$\delta_1-\delta_3$	1324.508	1321.703	1319.048	1316.255	1313.303	1310.623	1306.716	1302.706
	± 0.133	± 0.126	± 0.133	± 0.098	± 0.144	± 0.231	± 0.199	± 0.206
$\delta_3-\delta_7$	520.633	526.015	531.288	536.637	542.128	547.447	554.933	563.683
	± 0.148	± 0.144	± 0.154	± 0.114	± 0.145	± 0.238	± 0.199	± 0.220
D_{12}	−116.636	−108.536	−100.789	−93.356	−85.458	−77.912	−68.510	−57.308
	± 0.036	± 0.038	± 0.036	± 0.040	± 0.043	± 0.060	± 0.062	± 0.057
D_{13}	−15.595	−14.645	−13.698	−12.488	−11.674	−10.601	−9.288	−7.876
	± 0.065	± 0.068	± 0.065	± 0.066	± 0.064	± 0.104	± 0.078	± 0.083
D_{14}	−21.112	−20.274	−19.418	−18.481	−17.291	−16.031	−14.649	−12.786
	± 0.044	± 0.038	± 0.035	± 0.040	± 0.047	± 0.063	± 0.075	± 0.069
D_{15}	−37.699	−36.833	−35.574	−34.387	−32.712	−31.067	−28.539	−24.990
	± 0.037	± 0.040	± 0.033	± 0.036	± 0.046	± 0.061	± 0.054	± 0.069
D_{16}	15.697	13.846	12.080	10.540	9.109	7.925	6.098	4.664
	± 0.059	± 0.066	± 0.059	± 0.058	± 0.067	± 0.089	± 0.109	± 0.086
D_{17}[b]	68.614	65.612	62.162	58.829	55.153	51.284	46.116	39.96
	± 0.066	± 0.021	± 0.019	± 0.022	± 0.021	± 0.032	± 0.021	± 0.038
D_{18}[b]	11.899	10.742	10.212	9.433	8.760	8.097	7.155	5.983
	± 0.063	± 0.021	± 0.019	± 0.022	± 0.021	± 0.032	± 0.021	± 0.038
D_{36}	−26.983	−25.119	−23.178	−21.502	−19.748	−17.832	−15.740	−13.461
	± 0.068	± 0.059	± 0.077	± 0.061	± 0.060	± 0.154	± 0.094	± 0.109
D_{37}	−27.382	−24.747	−22.418	−20.334	−18.047	−16.050	−13.373	−10.891
	± 0.032	± 0.032	± 0.034	± 0.035	± 0.030	± 0.05	± 0.031	± 0.055
D_{78}	−359.313	−349.916	−339.041	−326.552	−311.471	−295.15	−270.586	−237.992
	± 0.053	± 0.062	± 0.064	± 0.069	± 0.062	± 0.082	± 0.054	± 0.077
rms	0.4	0.4	0.4	0.4	0.4	0.5	0.3	0.4

[a] See Figure 1 for the numbering. [b] In the spectral analysis, the strongly correlated values of D_{17} and D_{18} were constrained together. Only for the lower value of temperature was it possible to relax them during the very last iteration cycles (see text for explanations).

TABLE 4: Chemical Shifts Differences and Observed Residual Dipolar Couplings D_{ij}^{obs} (Hz) of NBD in the Liquid-crystalline Phase ZLI 1132[a] (sample 3)

T (K) T_{red}	309.0 0.90	312.4 0.91	315.8 0.92	319.3 0.93	322.7 0.94	326.1 0.95	329.6 0.96	333.0 0.97
$\delta_1-\delta_3$	1419.859	1413.989	1364.559	1359.66	1354.649	1349.315	1343.442	1336.737
	± 0.113	± 0.123	± 0.092	± 0.087	± 0.078	± 0.095	± 0.106	± 0.084
$\delta_3-\delta_7$	423.62	435.214	431.441	441.704	451.72	462.202	474.376	487.687
	± 0.125	± 0.125	± 0.091	± 0.091	± 0.078	± 0.101	± 0.111	± 0.089
D_{12}	−309.159	−290.862	−266.082	−249.993	−234.697	−218.376	−200.306	−181.118
	± 0.037	± 0.045	± 0.033	± 0.030	± 0.024	± 0.033	± 0.034	± 0.028
D_{13}	−39.207	−36.824	−33.767	−31.81	−29.925	−27.864	−25.515	−23.229
	± 0.053	± 0.053	± 0.038	± 0.036	± 0.032	± 0.046	± 0.051	± 0.041
D_{14}	−30.322	−29.201	−27.109	−26.035	−24.844	−23.537	−22.031	−20.289
	± 0.041	± 0.054	± 0.037	± 0.035	± 0.028	± 0.040	± 0.036	± 0.03
D_{15}	−30.334	−30.033	−28.937	−28.452	−27.93	−27.21	−26.096	−24.657
	± 0.039	± 0.050	± 0.035	± 0.036	± 0.026	± 0.039	± 0.036	± 0.028
D_{16}	74.146	68.851	62.369	57.943	53.803	49.496	44.807	39.996
	± 0.050	± 0.047	± 0.037	± 0.035	± 0.030	± 0.040	± 0.048	± 0.039
D_{17}[b]	117.151	112.329	100.671	98.687	93.67	88.272	82.023	75.176
	± 0.055	± 0.020	± 0.016	± 0.016	± 0.012	± 0.018	± 0.018	± 0.015
D_{18}[b]	28.709	26.419	24.661	23.087	21.89	20.382	18.603	16.946
	± 0.056	± 0.020	± 0.016	± 0.016	± 0.012	± 0.018	± 0.018	± 0.015
D_{36}	−72.565	−68.159	−62.29	−58.619	−54.957	−51.058	−46.927	−42.385
	± 0.058	± 0.061	± 0.041	± 0.04	± 0.036	± 0.044	± 0.052	± 0.037
D_{37}	−100.458	−93.761	−85.182	−79.48	−74.09	−68.502	−62.361	−55.931
	± 0.029	± 0.033	± 0.023	± 0.022	± 0.017	± 0.024	± 0.028	± 0.019
D_{78}	−297.819	−295.751	−283.546	−278.884	−272.993	−265.146	−254.024	−239.924
	± 0.07	± 0.067	± 0.051	± 0.051	± 0.038	± 0.051	± 0.054	± 0.038
rms	0.4	0.5	0.4	0.4	0.3	0.4	0.4	0.3

[a] See Figure 1 for the numbering. [b] In the spectral analysis, the strongly correlated values of D_{17} and D_{18} were constrained together. Only for the lower value of temperature was it possible to relax them during the very last iteration cycles (see text for explanations).

assigned lines (shortly called rms) are also given for each studied case: a noteworthy point, the quality of the spectral analysis is always very good, as testified by low rms and standard deviation values.

Besides the correct analysis of the spectrum, it is worth stressing that a "deceptive" interpretation could be achieved, even if the scalar couplings are fixed. The two solutions, characterized by sign-opposed sets of D_{ij} values and chemical shift differences, would lead to "mirror" orderings of the solute. It is possible to discriminate between the two possibilities by resorting to the relative magnitude of chemical shifts (known from standard isotropic experiment) or by intuitive (or "simulation-guided") physically sensible hypotheses about the solute preferred orientational order. About the NBD, the NMR studies in isotropic solutions ensure that the differences in chemical shifts between olefinic and alkylic protons are large enough to exclude the possibility of finding an inversion of sign due to chemical shift anisotropies. This allowed us a safe choice

between the two possible sets of D_{ij} values, and the choice was confirmed by simulations of the ordering of the "quasi-spherical" NBD (see the next sections).

4. Statement of the Problem

4.1. General Theory. The D_{ij}^{obs} term is given by the equation[1,2]

$$\forall i,j,\ D_{ij}^{obs} = -\mu_0 \gamma_i \gamma_j \frac{\hbar}{16\pi^2} \sum_{(a,b)\in\{x,y,z\}^2} \left\langle \frac{S_{ab} \cos\theta_{ij}^a \cos\theta_{ij}^b}{r_{ij}^3} \right\rangle \quad (1)$$

where $\hbar = h/2\pi$, with h being Planck's constant, γ the nuclear magnetogyric ratio, μ_0 the vacuum magnetic permeability, r_{ij} the $i-j$ internuclear distance, and θ_{ij}^a the angle between the a-axis of the molecular frame and the ij-direction. Special attention has to be drawn to the five independent S_{ab} order parameters, constituting the elements of the symmetric, real, and traceless Saupe matrix **S**: they are bearers of information about the ordering of the solute and their expression is given by

$$S_{ab} = \overline{(3\cos\theta_a{}^Z \cos\theta_b{}^Z - \delta_{ab})/2} \quad (2)$$

(here, δ is Krönecker's function and the upper bar denotes the orientational average over the overall rotation of the molecule, the so-called "molecular tumbling"[9]). Note that, knowing Saupe's parameters, it is possible to determine the order parameter S_{ij} of the axis passing through the ith and jth nuclei in the molecule by a simple orthogonal transformation

$$\forall i,j\ S_{ij} = \sum_{(a,b)\in\{x,y,z\}^2} S_{ab} \cos\theta_{ij}^a \cos\theta_{ij}^b \quad (3)$$

The explanation of the meaning of the symbol $\langle ... \rangle$ in eq 1 has been left as last, since it deserves quite a long digression. The angular brackets indicate averaging over any kind of internal molecular motion. About this, a conventional rough distinction is usually made between "flexible" and "rigid" molecules[2], where the latter are defined (according to a frequency-based classification) as "lacking of large-amplitude, low-frequency internal motions" (typically, but not only, the internal torsions). This definition, although quite effective, is not very rigorous, due to a certain arbitrariness in fixing the threshold between slow and fast motions. Another point of view, helpful in avoiding possible ambiguities, is to explicitly define as "rigid" the molecules lacking of subunits rotating with respect to one another (obviously, NBD belongs to this class): in this case, the only internal motions are represented by the sometimes called "hard" molecular vibrations, that is, bond stretchings and bond angle bendings. The observed dipolar couplings D_{ij}^{obs} can be formally partitioned as the sum of equilibrium dipolar couplings D_{ij}^{eq}, containing information about the "real" experimental equilibrium structure of the molecule, and D_{ij}^{vib} terms representing the "real" contribution to the dipolar couplings arising from the vibrational motion in the molecule

$$\forall i,j,\ D_{ij}^{obs} = D_{ij}^{eq} + D_{ij}^{vib} \quad (4a)$$

Of course, this relation is true within the experimental error affecting the D_{ij}^{obs} values and under the approximation of neglecting the J_{ij}^{aniso} contribution (see the previous section). In parallel, we can think to use a proper model to produce the so-called "calculated" dipolar couplings D_{ij}^{calc}

$$\forall i,j,\ D_{ij}^{calc} = D_{ij}^{ceq} + D_{ij}^{cvib} \quad (4b)$$

where D_{ij}^{ceq} and D_{ij}^{cvib} represent, respectively, the "calculated" partially averaged dipolar coupling between the ith and jth atom at the "equilibrium" state (i.e., the structure minimizing the electronic potential within the Born−Oppenheimer approximation) and the "calculated" vibrational correction. Once we dispose of eqs 4a and 4b, it is obviously possible to write the theoretical differences $\Delta_{ij}^T = (D_{ij}^{calc} - D_{ij}^{obs}) = \Delta_{ij}^{eq} + \Delta_{ij}^{vib}$ (where $\Delta_{ij}^{eq} = (D_{ij}^{ceq} - D_{ij}^{eq})$ and $\Delta_{ij}^{vib} = (D_{ij}^{cvib} - D_{ij}^{vib})$). In principle, these differences should be minimized as much as possible, in particular trying to make them smaller than the standard deviations on the data; in practice, such a high level of success in reproducing the D_{ij}^{obs} set of couplings is hardly ever achieved. Looking at the expression of the differences as a sum of Δ_{ij}^{eq} and Δ_{ij}^{vib} contributions, it is immediately realized that the discrepancies between the observed and calculated couplings can be thought as arising not only by an imperfect reproduction of the set of "equilibrium" dipolar couplings (from which an "equilibrium" molecular geometry should be extracted) but also by errors in reproducing the "real" effect of vibrations. Of course, the single role of each of the two terms contributing to the whole Δ_{ij}^T cannot be in principle disentangled: the consequences of this fact will be discussed further in the paper. It should be emphasized that eq 1, in that form, reckons with considering the weak (but existing) orientation−vibration coupling mechanisms and is in practice unusable as it stands, since it would imply the ability to evaluate an order matrix for each vibrational state involved in the averaging $\langle ... \rangle$ process.[10] To make the problem manageable, the correlation between molecular vibrations and reorientational motion was tackled some years ago, by using approximations;[10,11] anyway, the problem is still living and topical, as testified by a very recent work concerning ethane and its isotopomers.[11j] In the present context, we will refer to the framework of the problem suggested by Lounila and Diehl (LD). In the LD approximated theory,[11f−h] the explicit form of the D_{ij}^{vib} term results in

$$D_{ij}^{vib} \approx D_{ij}^{h} + D_{ij}^{a} + D_{ij}^{d} + D_{ij}^{hp} \quad (5)$$

where D_{ij}^{h} and D_{ij}^{a} arise, respectively, from the unperturbed harmonic vibrations and the anharmonic vibrations due to the cubic terms[11h] (higher order terms are neglected), whereas D_{ij}^{d} and D_{ij}^{hp} originate, respectively, from molecular deformations and harmonic perturbations of vibrations due to orientation-dependent anisotropic forces and their gradients (second-order theory for the molecular motions).[11h] The LD theory (as the other suggested approaches), even though approximated, implies quite complicated calculations; so, for convenience (or "conventionally", as said by Lounila and Diehl in ref 11f), the calculations are commonly carried out by assuming de facto the decoupling of internal and reorientational motions.[2] Under this approximation, eq 1 assumes the following simplified form

$$\forall i,j,\ D_{ij}^{obs} \approx -\mu_0 \gamma_i \gamma_j \frac{\hbar}{16\pi^2} \sum_{(a,b)\in\{x,y,z\}^2} \langle S_{ab} \rangle \left\langle \frac{\cos\theta_{ij}^a \cos\theta_{ij}^b}{r_{ij}^3} \right\rangle \quad (6)$$

Strictly speaking, if the decouplings were "exact" (and not an approximation), then the S_{ab} elements should be really vibration-independent.[10] Since, in our case, this is only an approximation, the resulting order parameters $\langle S_{ab} \rangle$ are kind of "effective", "vibrationally averaged" order parameters resulting from the

experimental data:[1] henceforth, the "vibrationally averaged" order parameters $\langle S_{ab} \rangle$ will be indicated simply as S_{ab}. As a consequence of the "pragmatic" reorientation−vibration decoupling, D_{ij}^{vib} becomes

$$D_{ij}^{vib} \approx D_{ij}^{h} + D_{ij}^{a} \tag{7}$$

From the comparison between eq 5 and eq 7, it is possible to realize that the two last terms of eq 5 (D_{ij}^{d} and D_{ij}^{hp}) vanish upon passing from the coupled orientation−vibration description (although treated in an approximate way) to the fully decoupled description. Particular attention should be given to the disappearance of D_{ij}^{d}: in the framework of the LD theory, it contains the information about distortions induced by the solvent on the equilibrium structure of the solute; therefore, the use of eq 6 (the decoupled form) with the consequent expression 7 for D_{ij}^{vib} (where only the harmonic and anharmonic terms survive) precludes in principle the direct theoretical access to possible deformations induced by the solvent. This seems to be a severe drawback to the use of eq 6; anyway, it should be stressed that the use of eq 6 rather than eq 1 could have significant consequences only when subtle solvent effects[11] on the LXNMR-determined structures are investigated (about this point, see refs 11j and 12 and references therein). On the other hand, if the aim of the study requires a very high accuracy, then the J_{ij}^{aniso} term cannot be ignored anymore, so it has to be reintroduced in the treatment besides the four terms of eq 5 (see, for example, ref 13 and references therein). In practice, the adoption of the simpler eq 6 and (consequently) eq 7 is quite effective and successful in most cases, and in any case, possible solvent-induced effects and/or significant reorientation−vibration interactions can be inferred in an indirect way, from "clues" due to bad or unsatisfactory or inexplicable or contradictory results.[11j] Following the argument given above, in this work, we chose to use eqs 6 and 7; moreover, since the harmonic term constitutes by far the largest contribution to the vibrational corrections, the usual assumption to drop D_{ij}^{a} in eq 7 has been adopted.[14] The observed dipolar couplings then became

$$\forall i,j,\ D_{ij}^{obs} = D_{ij}^{eqs} + D_{ij}^{h} \tag{8}$$

where D_{ij}^{eqs} represents an "effective" dipolar coupling corresponding, from a physical point of view, to the "experimental" equilibrium dipolar coupling if the vibrational corrections were strictly due to the harmonic terms only. The D_{ij}^{h} values are exclusively dependent upon the nature of the force field (FF) used, the IR vibrational frequencies of the solute, and the temperature of the experiment.[15] The FF can be derived experimentally, from the analysis of a vibrational spectrum or, as more recently done with good results, calculated by some high-level ab initio or density functional method.[16−18]

The choice of adopting eq 8 rather than eq 4a and the $D_{ij}^{vib} = D_{ij}^{h}$ position, automatically imply that $D_{ij}^{eqs} = D_{ij}^{eq}$. All the approximations adopted to simplify the treatment of the problem certainly introduce a (hopefully small) additional term Δ_{ij}^{approx} to the above-mentioned theoretical error Δ_{ij}^{T}, so that the real discrepancies in reproducing the experimental data are given by $\Delta_{ij} = \Delta_{ij}^{T} + \Delta_{ij}^{approx}$. Since an exact assessment of the magnitude of Δ_{ij}^{approx} is impossible, the "philosophy" of adopting approximations suggests to neglect it; anyway, one should be aware that all the conclusions that can be drawn about the studied system are affected by the Δ_{ij}^{approx} term and an a posteriori qualitative estimate of the effects of Δ_{ij}^{approx} can be attempted.

4.2. Solute−Solvent Orientational Interaction. The use of ^{1}H-LXNMR of small solutes dissolved in nematic phase can be very useful to try to gather the "essence" about the nature of mechanisms underlying the liquid crystal orientational phenomena (responsible for the very peculiar properties of liquid crystals that make them so interesting, not only from a fundamental but also from a technological point of view). Describing or predicting this ordering is not an easy task, as testified by the large number of existing theories and models conceived to treat the problem.[2] To do this, it can be useful to express order parameters exploiting equilibrium statistical mechanics[10]

$$\forall a,b,\ S_{ab} = \frac{\int (3\cos\theta_a^{Z}\cos\theta_b^{Z} - \delta_{ab}) \exp(-U(\beta,\gamma)/k_B T)\sin\beta\, d\beta\, d\gamma)}{2\int \exp(-U(\beta,\gamma)/k_B T)\sin\beta\, d\beta\, d\gamma} \tag{9}$$

where β and γ are the Euler angles giving the orientation of the director in the molecular frame. In this formula, the attention moves at once at $U(\beta,\gamma)$, the anisotropic potential describing the orientational solute−solvent interaction. Often this potential is thought as the superposition of two effects, the first being a shape- and steric-hindrance-based effect, modeled as a short-range contribution $U_{sr}(\beta,\gamma)$, and the second, a long-range term $U_{lr}(\beta,\gamma)$

$$U(\beta,\gamma) = U_{sr}(\beta,\gamma) + U_{lr}(\beta,\gamma) \tag{10}$$

A possible way to describe this potential is that proposed by Celebre[19,20] a few years ago and successfully used in the recent past for several systems.[21,22] In the frame of this model, $U_{sr}(\beta,\gamma)$ is described modeling the solute as a parallelepipedal box surrounded by the anisotropic medium, whereas the long-range effects are mainly attributed to electrostatic interactions between an average EFG of the solvent and the solute's electric quadrupole moment. About $U_{lr}(\beta,\gamma)$, it is worth emphasizing that, in principle, also possible orientational mechanisms due to the existing solute's dipole moment should be taken into account. Anyway these effects, extensively studied in the recent past for other molecules (see, e.g., refs 25 and references therein), resulted as always very small and elusive, leading to the quite commonly accepted conclusion that the role of the molecular dipole moment in the long-range orientational interactions can be considered negligible. Moreover, if the magnitude of the dipole moment of NBD is very small (μ = 0.05867 D),[24b] then even more so it can be safely neglected in our study.

4.2.1. Modeling of $U_{sr}(\beta,\gamma)$. As said above, in the used model, the solute is thought as a hard rectangular block whose dimensions are evaluated by taking into account the atomic positions in the molecule and the van der Waals radii for each atom,[23] whereas the solvent is partitioned into two regions. The first one, occupied by the nearest neighbors of the solute, is described as a face centered lattice of six cylindrically shaped solvent-like molecules. Their orientations in the molecular PAS frame are randomly generated around the parallelepiped, using a random number generator based on L'Ecuyer's algorithm with Bays−Durhem shuffle (see refs 19−21 for computational details). These six molecules mimic the first layer of solvation (the direct environment) and therefore model the local solute−solvent interactions, thus mostly depending on the size and shape of the solute. A macroscopic, "mean-field" vision is on the

contrary adopted to model the bulk of the solvent. Indeed, a detailed description of the very large number of solvent molecules far away from the solute is probably not necessary to get a rough (but realistic) contribution to the orientation of the solute, since such interactions contribute mainly to the overall solvent order. On the other hand, such a simulation of the bulk could be especially time-consuming (without great advantages) when modeled as a statistically significant number of solvent molecules interacting with each other. The rest of the medium is hence described through a virtual phase director (resulting from the auto-organization of the more distant solvent molecules), whose instantaneous orientation in the solute molecular frame is randomly generated step-by-step by using a metropolis/MC procedure. Finally

$$U_{sr}(\beta,\gamma) = -\frac{\epsilon k_B T}{6}\sum_{j=1}^{6} F_j \sigma_j \sum_j \qquad (11)$$

where ϵ is the orientational energy expressed by length unit, F_j is the dimension of jth face of the solute's modeling box, and σ_j and Σ_j are given by

$$\sigma_j = (3\cos^2\varphi_j - 1)/2 \qquad (12)$$

$$\sum_j = (3\cos^2\Theta_j - 1)/2 \qquad (13)$$

where φ_j is the angle between the jth nearest neighbor solvent molecule and the jth molecular system axis (the sum of eq 11 over the six faces of the box runs two times over x-, y-, and z-directions) and Θ_j is the angle between the jth nearest neighbor solvent molecule and the director.

4.2.2. Modeling of $U_{lr}(\beta,\gamma)$. As the electric quadrupole moment of the solute is a molecular property, the components of the second-rank tensor associated may be experimentally measured[24a] or obtained by theoretical calculations.[22,25a] The explicit expression used for modeling $U_{lr}(\beta,\gamma)$ is[22]

$$U_{lr}(\beta,\gamma) = -\frac{1}{2}F_{ZZ}(Q_{zz}\cos^2\beta + (Q_{xx}\cos^2\gamma + Q_{yy}\sin^2\gamma)\sin^2\beta) \qquad (14)$$

where **Q** is the symmetric traceless quadrupolar tensor given in the molecular frame and F_{ZZ} formally represents the ZZth component of the average EFG of the nematic solvent "felt" by the solute (note that, due to the NBDs symmetry, the PAS of the **Q** tensor coincides with that of the **S** matrix, shown in Figure 1).

5. Determination of NDBs Geometry and Order Parameters

Equation 6 states that D_{ij}^{obs} contains information about the solute's orientational order (via S_{ab}) and geometry (via the piece $\langle\cos\theta_{ij}^a \cos\theta_{ij}^b/r_{ij}^3\rangle$ where, also noteworthy, the vibrational corrections are involved). So, in principle, eq 6 could represent a useful tool to study the structure and the ordering of the probe dissolved in the mesophase. On the other hand, it is simple to realize that the two "ingredients" are "interdependent" in the sense that the setting of one of them "modulates" the value of the other, to reproduce the experimental dipolar couplings. In the following, for convenience and for the sake of clarity, we will discuss separately the geometry and orientational order of NBD, although, of course, the determination of both the "ingredients" was carried out at the same time.

5.1. On the Structure of NBD in the Nematic Solutions. Being, at the start, that the values of S_{ab} were totally unknown, it follows that, to determine experimental order parameters from partially averaged dipolar couplings, a choice of the solute's geometry is required. Several old and recent works exist about NBDs geometries, studied both theoretically[26,27] and experimentally (by X-ray diffraction (XD),[28,29] electron diffraction (ED),[30,31] MW,[32] and LXNMR[8,33,34]); so, a wide "spectrum" of possible choices is offered by the literature. On the other hand, as said above, the choice is far from being "neutral", since it inevitably affects the orientational results (see eq 6). This is not a new problem;[35] anyway, in the present context, it represents a delicate point deserving some comments. First of all, it should be emphasized that the state of matter can turn out to be important: in principle (but not necessarily), the geometries are phase-dependent and those calculated "in vacuo" and/or obtained by gas-phase experiments (where we refer to the "isolated" molecule) could differ from those determined (by other experimental techniques) in the liquid and/or solid phase, where the molecule significantly interacts with its environment. Moreover, if we consider fluid condensed (liquid) phases, then it is (in principle) possible to observe differences in structural results obtained (by the same technique, LXNMR in particular) in different solvents: in this case, we speak about "solvent effects" (by reversing the argument, the finding of a "common" geometry, good for different solvents, could be a "clue" of no solvent effects). Other problems are nested into the search of solvent effects, namely, (a) the use of eq 6 rather than eq 1 can be misleading (it can be shown[11h] that possible deformational effects induced by the solvent can be explicitly taken into account only by using eq 1; otherwise, solvent-induced effects can be "inferred" in an "indirect" way, from clues due to bad or ambiguous or controversial results); (b) as said above, the vibrational contributions to the observed dipolar couplings have to be taken into account. The need of application of vibrational corrections[14a,15] implies further (not necessarily "aseptic") choices, as, for example, the choice of the best force field (empirical or calculated and, if calculated, by which method), the use of IR frequencies (experimental or calculated), and so forth. About this point, in the present work, vibrational corrections have always been calculated by density functional theory (DFT) method B3LYP/6-31++G** (this method is believed to be very reliable[36] in predicting vibrational FFs[16]) and using experimental[26] and calculated frequencies (also, in this case, as found in past studies,[17] only negligible differences have been found when using experimental instead of calculated vibrational frequencies). Technically speaking, the calculations have been carried out by making use of the AnCon package,[37] an "all-inclusive" homemade friendly graphic interface for the whole processing of LXNMR data (AnCon is also designed to share geometry input files with standard quantum-mechanics software packages and to acquire calculated FFs to be used in the data treatment). We started by testing geometries from previous LXNMR studies[8,33,34] (two of those[8,34] carried out in EBBA, one of the solvents here used; see the Experimental section), but we realized soon that none of the geometries from past studies were "directly" suitable as the *optimum* common geometry for the three solvents (i.e., able to reproduce, very well and simultaneously, the whole set of data in the three mesophases). In particular, for NBD in EBBA only, we found, as expected, quite good values of the error function R (where $R = (\sum_{k=1}^{N}\Delta_k^2/N)^{1/2}$, with N = number of dipolar couplings), ranging with temperature from ~0.5 to ~0.2 Hz. On the contrary, in MM, the R values were not very low (~1.1/~0.7

TABLE 5: NBDs Geometries in Cartesian Coordinates (see PAS framework from Figure 1)[a]

	x_1/Å	y_1/Å	z_1/Å	x_3/Å	y_3/Å	z_3/Å	x_7/Å	y_7/Å	z_7/Å
B3LYP/6-31++G**	1.936	1.339	0.000	0.000	−2.161	1.633	0.900	0.000	3.000

[a] The coordinates of H_1, H_3, and H_7 are reported, while those of the other hydrogen atoms can be immediately obtained by using the C_{2v} symmetry properties of the solute.

TABLE 6: "Equilibrium", Calculated, and Observed Dipolar Couplings; Harmonic Vibrational Corrections, Deviations, Relative Corrections, and *R* for NBD at $T_{red} = 0.94$ in EBBA, MM, and ZLI1132 (geometry and FF by B3LYP/6-31++G; experimental frequencies used in evaluating vibrational corrections; see text for more explanations)[a]**

		D_{ij}^{ceq} [b]	D_{ij}^{h} [c]	D_{ij}^{calc} [d]	D_{ij}^{obs} [e]	Δ[f]	corr[g]
				NBD in EBBA			
$T_{red} = 0.94$ ($T = 319.0$ K)	D_{12}	54.229	−0.2557	53.9729	53.7920	0.1809	−0.0048
	D_{13}	4.241	−0.0089	4.2317	4.6360	−0.4043	−0.0019
	D_{14}	−18.302	0.0977	−18.2040	−18.2930	0.0890	−0.0053
	D_{15}	−57.191	−0.0584	−57.2495	−58.8800	1.6305	0.0010
	D_{16}	−42.324	−0.0551	−42.3795	−43.1500	0.7705	0.0013
	D_{17}	38.797	−0.1031	38.6942	38.8390	−0.1448	−0.0027
	D_{18}	−2.811	−0.0529	−2.8635	−2.5330	−0.3305	0.0209
	D_{36}	12.885	−0.0561	12.8294	13.5650	−0.7356	−0.0041
	D_{37}	43.917	−0.3699	43.5468	43.1370	0.4098	−0.0086
	D_{78}	−569.336	18.4107	−550.9250	−550.4450	−0.4800	−0.0334
	R	0.61					
				NBD in MM			
$T_{red} = 0.94$ ($T = 314.4$ K)	D_{12}	−93.767	0.9215	−92.8451	−93.3560	0.5109	−0.0099
	D_{13}	−12.882	0.0926	−12.7897	−12.4880	−0.3017	−0.0074
	D_{14}	−18.364	0.0531	−18.3113	−18.4810	0.1697	−0.0029
	D_{15}	−33.960	0.0182	−33.9415	−34.3870	0.4455	−0.0005
	D_{16}	10.784	0.2106	10.9950	10.5400	0.4550	0.0200
	D_{17}	58.974	−0.2197	58.7546	58.8290	−0.0744	−0.0037
	D_{18}	9.650	−0.1123	9.5379	9.4330	0.1049	−0.0119
	D_{36}	−22.280	0.0892	−22.1912	−21.5020	−0.6892	−0.0041
	D_{37}	−20.163	−0.3394	−20.5028	−20.3340	−0.1688	0.0167
	D_{78}	−338.068	11.2708	−326.7975	−326.5520	−0.2455	−0.0345
	R	0.32					
				NBD in ZLI1132			
$T_{red} = 0.94$ ($T = 324.0$ K)	D_{12}	−235.661	2.1105	−233.5510	−234.6970	1.1460	−0.0090
	D_{13}	−29.999	0.1996	−29.7991	−29.9250	0.1259	−0.0067
	D_{14}	−24.726	0.0383	−24.6875	−24.8440	0.1565	−0.0015
	D_{15}	−28.425	0.0813	−28.3441	−27.9300	−0.4141	−0.0029
	D_{16}	53.842	0.4798	54.3216	53.8030	0.5186	0.0089
	D_{17}	94.203	−0.3817	93.8217	93.6700	0.1517	−0.0041
	D_{18}	22.201	−0.1949	22.0061	21.8900	0.1161	−0.0089
	D_{36}	−55.997	0.2275	−55.7692	−54.9570	−0.8122	−0.0041
	D_{37}	−74.574	−0.4335	−75.0080	−74.0900	−0.9180	0.0059
	D_{78}	−282.974	9.8566	−273.1174	−272.9930	−0.1244	−0.0361
	R	0.55					

[a] All dimensional values are given in hertz. [b] Partially averaged dipolar couplings values calculated for the molecule at its equilibrium state. [c] Vibrational motion contribution to be added to D^{ceq} values. [d] $D^{calc} = D^{ceq} + D^{h}$. [e] Partially averaged dipolar couplings values observed. [f] $\Delta = D^{calc} - D^{obs}$. [g] corr $= D^{h}/D^{obs}$.

Hz) and unacceptably high for NBD in ZLI1132 (∼2.4/∼1.7 Hz). Only after optimization of the geometries (see Table SI-1 in the Supporting Information, where the starting and optimized geometries, fixing the H_7H_8 distance at 1.82 Å from ref 8, are reported) with the resulting "solvent-tailored" geometries did we obtain a very good reproduction of experimental data (typical *R*, EBBA ∼ 0.3 Hz; MM ∼ 0.4 Hz; ZLI1132 ∼ 0.3 Hz). Subsequently, when the B3LYP/6-31++G** geometries calculated by the GAUSSIAN 03 package[38] were used (Table 5), we found at once a good agreement in reproducing simultaneously the whole set of dipolar couplings for NBD in the three solvents at different temperatures (of course, with the proper order parameters; see the next section) without any change or adjustment.

As an example, dipolar coupling values, vibrational harmonic corrections obtained by using experimental frequencies,[26] and *R* values, together with other useful information, are reported in Table 6 for a single temperature corresponding to $T_{red} = 0.94$. The same data for all the temperatures are reported in Tables SI-2, SI-3, and SI-4 of the Supporting Information, respectively, for the solute in EBBA, MM, and ZLI1132. It is worth emphasizing that the calculated vibrational corrections, less than 3% at most, do not exceed the usual magnitude expected for proton−proton dipolar couplings,[1,14a,15] even if the absolute magnitude of dipolar couplings are quite small, due to the "quasi-spherical" shape of NBD. As reported in Tables SI-2, SI-3, and SI-4, when the temperature is changed, the found *R* values span from ∼0.7 to ∼0.4 Hz in EBBA, from ∼0.3 to ∼0.2 Hz in MM, and from ∼0.6 to ∼0.4 Hz in ZLI1132; whereas $\bar{R} = (1/N_{exp}) \sum_{Ti} \sum_{Solv_i} R_{Ti}^{Solv_i}$, that is, the *R* value averaged over all the temperatures and the used solvents (with $N_{exp} = 24$ in our case), is calculated at 0.5 Hz. Other theoretical geometries (vibrationally corrected by using the B3LYP-calculated FF) have been tested (see Table 7, where NBD

TABLE 7: NBDs Geometrical Distances (in angstroms) and Ratios (see Figure 1 for atom numbering)

	r_{12}	r_{15}	r_{16}	r_{17}	r_{36}	r_{67}	r_{78}	r_{12}/r_{36}	r_{15}/r_{36}	r_{16}/r_{36}	r_{17}/r_{36}	r_{67}/r_{36}	r_{78}/r_{36}
B3LYP 6-31++G**	2.678	3.872	2.663	3.445	4.322	2.711	1.800	0.620	0.896	0.616	0.797	0.627	0.416
LSDA 6-311++G**	2.676	3.830	2.656	3.424	4.310	2.695	1.818	0.621	0.889	0.616	0.794	0.625	0.422
RHF/6-31G**	2.640	3.864	2.648	3.417	4.284	2.690	1.780	0.616	0.902	0.618	0.798	0.628	0.415
from ref 8	2.708	3.826	2.639	3.456	4.384	2.758	1.820	0.618	0.873	0.602	0.788	0.629	0.415
from ref 33 (in EBBA)	2.694	3.816	2.633	3.473	4.384	2.773	1.816	0.615	0.870	0.601	0.792	0.633	0.414
from ref 33 (in phase IV)	2.624	3.706	2.571	3.351	4.384	2.732	1.752	0.599	0.845	0.586	0.764	0.623	0.400
EBBA[a] ($T_{red} = 0.94$)	2.700	3.834	2.641	3.455	4.346	2.739	1.820	0.621	0.882	0.608	0.795	0.630	0.419
MM[a] ($T_{red} = 0.94$)	2.686	3.874	2.682	3.458	4.374	2.734	1.820	0.614	0.886	0.613	0.791	0.625	0.416
ZLI1132[a] ($T_{red} = 0.94$)	2.690	3.882	2.675	3.460	4.356	2.732	1.820	0.618	0.891	0.614	0.794	0.627	0.418
EBBA[b] ($T_{red} = 0.94$)	2.680	3.817	2.631	3.429	4.322	2.703	1.793	0.620	0.883	0.609	0.793	0.625	0.415
MM[b] ($T_{red} = 0.94$)	2.646	3.831	2.644	3.415	4.322	2.704	1.785	0.612	0.886	0.612	0.790	0.625	0.413
ZLI1132[b] ($T_{red} = 0.94$)	2.664	3.855	2.655	3.435	4.322	2.706	1.791	0.616	0.892	0.614	0.795	0.626	0.414

[a] Optimized, H_7-H_8 distance kept fixed to 1.82 Å (ref 8). [b] Optimized, H_3-H_6 distance kept fixed to 4.32 Å (from B3LYP/6-31++G**).

distances and distance ratios for the different used geometries are reported), with quite good (but not excellent) agreement with the data (LSDA/6-311++G**, $R \sim 1.5$ Hz; RHF/6-31G**, $R \sim 0.9$).

If we look only to the reasonably low value of $\bar{R}$, the discussion carried out above should lead quite safely to the conclusion that (under the approximations adopted in this treatment and in the limits allowed by the goodness of the experimental D_{ij} values fittings) the B3LYP/6-31++G** geometries well describe a temperature-independent structure assumed by the NBD molecule when dissolved in any of the tested solvents (irrespective of the specific nature of the nematic medium). What is found, in our opinion, is even more intriguing because, at present, there is a renewed interest to the "classical" problem of solvent-induced effects on small molecules dissolved in nematic solvents (or, that is, the same, about the "reliability" of LXNMR-determined structures). This is testified by very recent papers about the topic[12,39] (as an example, a very recent work, carried out on iodomethane dissolved in three different nematic phases—EBBA, ZLI1132, and I52—using the variable angle spinning NMR, concluded that "the apparent bond angle deviations (...) arise from a solvent effect and are not an artifact from scaling the anisotropic interactions").[39] Our present study fits quite well in this scientific context and the results we achieved lend themselves to interesting considerations, in particular when compared with the already cited LXNMR old studies,[8,33,34] carried out in EBBA and phase IV. In the case of NBD, if the solvent-induced structural deformations were weak enough to be disregarded, some ratios between "equilibrium" experimental dipolar couplings D_{ij}^{eq} values, in particular D_{15}^{eq}/D_{78}^{eq} (or equally D_{24}^{eq}/D_{78}^{eq}) and D_{36}^{eq}/D_{12}^{eq} (or equally D_{36}^{eq}/D_{45}^{eq}), should be independent of the orientation of the molecule, whatever the solvent used. This happens because, due to the C_{2v} symmetry of the solute (see Figure 1), as the axes r_{78} and r_{15} (or r_{24}) as r_{36} and r_{12} (or r_{45}) are parallel, so they should possess the same orientational parameters: $S_{78} = S_{15} = S_{24}$ and $S_{36} = S_{12} = S_{45}$.[1] This fact, in turn, implies that, exploiting eqs 3, 6, and 8, it is possible to write the following relations

$$D_{15}^{eq}/D_{78}^{eq} = r_{78}^3/r_{15}^3$$

$$D_{36}^{eq}/D_{12}^{eq} = r_{12}^3/r_{36}^3 \qquad (15)$$

The old LXNMR studies (carried out by taking into account vibrational corrections) did not find the invariance of the above-mentioned ratios upon passing from EBBA to phase IV (they found changes of about 1% and 17%[1] respectively, for the two ratios reported above). This kind of behavior was recognized as a "symptom" of solvent-induced effects on the solute, so

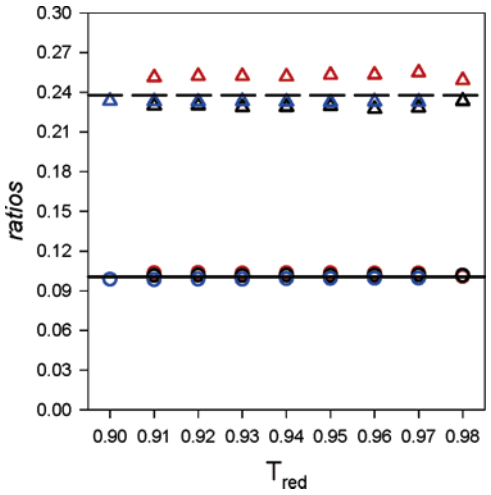

Figure 4. Behavior of $D_{15}^{eqs}/D_{78}^{eqs}$ (circles) and $D_{36}^{eqs}/D_{12}^{eqs}$ (triangles) ratios vs T_{red} in the three different nematic solvents (red, EBBA; black, MM; blue, ZLI1132), compared with theoretical values of B3LYP/6-31++G**-geometries calculated ratios r_{78}^3/r_{15}^3 (solid line) and r_{12}^3/r_{36}^3 (dashed line).

authorizing the conclusion that NBD has different structures in the two nematogens.[1] Our present results are shown in Figure 4, where the ratios $D_{15}^{eqs}/D_{78}^{eqs}$ (or equally $D_{24}^{eqs}/D_{78}^{eqs}$) and $D_{36}^{eqs}/D_{12}^{eqs}$ (or equally $D_{36}^{eqs}/D_{45}^{eqs}$) in the three liquid-crystalline solvents vs the reduced temperature of NMR experiments are reported. In the same figure, two lines are also drawn, marking the values of the corresponding theoretical ratios (r_{78}^3/r_{15}^3 and r_{12}^3/r_{36}^3) from B3LYP/6-31++G** geometries.

It should be emphasized that the $D_{lk}^{eqs}/D_{mn}^{eqs}$ ratios (and not the "true" D_{lk}^{eq}/D_{mn}^{eq} ratios) are plotted in the figure. The relation linking the two ratios is the following (see section 4.1)

$$\frac{D_{lk}^{eqs}}{D_{mn}^{eqs}} = \frac{D_{lk}^{eq} + (\Delta_{lk}^{eq})}{D_{mn}^{eq} + (\Delta_{mn}^{eq})} = \frac{D_{lk}^{eq} + (\Delta_{lk}^{T} - \Delta_{lk}^{vib} - \Delta_{lk}^{approx})}{D_{mn}^{eq} + (\Delta_{mn}^{T} - \Delta_{mn}^{vib} - \Delta_{mn}^{approx})} \qquad (16)$$

where also the relation $\Delta_{ij}^{eq} = \Delta_{ij}^{T} - \Delta_{ij}^{vib} - \Delta_{ij}^{approx}$ has been used (of course, in this notation, the errors are inclusive of the signs). In our opinion, eq 16 is useful because the possible causes of discrepancies explicitly appear. In particular, Δ_{ij}^{T} contains the information about the quality of the reproduction of the experimental datum (it is a function reflecting the $\bar{R}$ goodness of the whole fitting); Δ_{ij}^{vib} ideally represents the wrong way to describe vibrational corrections; finally, Δ_{ij}^{approx} is a kind of "black box" where the effects (difficult to quantify exactly) of all the approximations adopted to simplify the treatment of the problem have been discharged. Looking at Figure 4, with the

exception of the $D_{36}^{eqs}/D_{12}^{eqs}$ ratio of NBD in EBBA, we can maintain that the agreement between the symbols and the lines predicted by the B3LYP-calculated geometrical ratios is excellent. As said above, the only behavior significantly different from the theoretical trend (but always within ~5% of variation only) concerns the $D_{36}^{eqs}/D_{12}^{eqs}$ ratio of NBD in EBBA. We think this is a too weak evidence to conclude that EBBA "distorts" the geometry of the molecule, also because (in light of the considerations carried out above) the slight deviation observed could be, at least partly, due to the "inscrutable" effects of Δ_{ij}^{vib} and Δ_{ij}^{approx}. Further terms in describing the vibrational corrections (taking into account, if possible, anharmonic terms and reorientational−vibrational correlation) and/or the reintroduction of the $(1/2)J_{ij}^{aniso}$ term in the expression of the direct couplings and/or a more accurate determination of scalar couplings (usually, as in this case, the J_{ij}^{iso} values are generically assumed from previous studies and kept fixed) could contribute to improve the alignment of the lines and symbols. A detailed treatment of these quite complicated aspects is out of the scope of this paper; anyway, developments in the indicated directions are at present in progress in our laboratory. Before concluding the discussion of our results, and to avoid misunderstanding, we would like to emphasize an aspect that, to our knowledge, has been never raised in previous studies: the invariance of the significant dipolar coupling ratios to assess possible solvent-induced deformations **is a necessary but not a sufficient condition** to affirm that the theoretical molecular geometry holds. This can be mathematically demonstrated in a very simple way. By trivial algebra, eq 16 can be usefully rearranged in the following manner

$$\frac{D_{lk}^{eqs}}{D_{mn}^{eqs}} = \frac{D_{lk}^{eq}}{D_{mn}^{eq}} \frac{(1+\delta_{lk}^{eq})}{(1+\delta_{mn}^{eq})} \tag{17}$$

where $\delta_{lk}^{eq} = \Delta_{lk}^{eq}/D_{lk}^{eq}$ and $\delta_{mn}^{eq} = \Delta_{mn}^{eq}/D_{mn}^{eq}$ represent the relative errors on the "real" equilibrium couplings. By exploiting eq 15 and eq 17, we can write

$$\frac{D_{36}^{eqs}}{D_{12}^{eqs}} = \frac{r_{12}^3}{r_{36}^3} \frac{(1+\delta_{36}^{eq})}{(1+\delta_{12}^{eq})}; \frac{D_{15}^{eqs}}{D_{78}^{eqs}} = \frac{r_{78}^3}{r_{15}^3} \frac{(1+\delta_{15}^{eq})}{(1+\delta_{78}^{eq})} \tag{18}$$

From eq 18, it is immediate to realize that when the ratio $(1+\delta_{lk}^{eq})/(1+\delta_{mn}^{eq}) \rightarrow 1$, then $D_{lk}^{eqs}/D_{mn}^{eqs} \rightarrow r_{mn}^3/r_{lk}^3$. This happens of course not only (and this is the "regular" case) when $\delta_{lk}^{eq} \rightarrow 0$ and $\delta_{mn}^{eq} \rightarrow 0$ simultaneously (in this case, eq 17 sets that D_{lk}^{eqs} and D_{mn}^{eqs} coincide with D_{lk}^{eq} and D_{mn}^{eq}, respectively) but also when $\delta_{lk}^{eq} = \delta_{mn}^{eq}$. In this second ("pathological") case, the relative error δ_{lk}^{eq} on the corresponding dipolar coupling could be also very large, but it suffices that δ_{mn}^{eq} is about the same to ensure that $D_{lk}^{eqs}/D_{mn}^{eqs} \approx r_{mn}^3/r_{lk}^3$.

Following what expounded above (and in light of the approximations and assumptions adopted in the work), we cannot claim to have furnished the incontrovertible "proof" that the NBDs structure is undistorted and solvent-independent. Strictly speaking (and without generalizing), we can only state that the dipolar coupling information content is compatible (within a 5% error, at most) with a NBDs geometry which, compared with the "in vacuo" calculated structure, is not affected in a significant way (or, better, beyond any reasonable doubt) by the tested solvents. Of course, we cannot exclude in principle that the "true" equilibrium geometries of NBD in the different nematic phases are those slightly "distorted" (and different for each solvent) that we reported in Table 7 and in Table SI-1 of the Supporting Information; anyway, this kind of conclusion could be considered at least quite rash. Finally, a further refining of B3LYP/6-31++G** geometries improved (as obviously expected) the fittings ($R \leq 0.2$ for all the solvents and temperatures), but the changes were so slight (less than 0.3%) to be safely considered in the range of experimental error. So, to make the least biased choice, we decided to adopt the "intact" B3LYP/6-31++G** geometries as our final set.

TABLE 8: Experimental "equilibrium" S_{zz} and $S_{xx} - S_{yy}$ Values (estimated error on the values, ±1%)

	EBBA		MM		ZLI 1132	
T_{red}	S_{zz}	$S_{xx} - S_{yy}$	S_{zz}	$S_{xx} - S_{yy}$	S_{zz}	$S_{xx} - S_{yy}$
0.90					−0.065	−0.0346
0.91	−0.0209	0.0409	−0.0368	−0.0007	−0.0616	−0.0318
0.92	−0.0203	0.0394	−0.0350	0.0002	−0.0567	−0.0283
0.93	−0.0197	0.0379	−0.0332	0.0009	−0.0541	−0.0260
0.94	−0.0190	0.0363	−0.0314	0.0014	−0.0514	−0.0239
0.95	−0.0181	0.0344	−0.0294	0.0019	−0.0484	−0.0217
0.96	−0.0172	0.0324	−0.02735	0.0023	−0.0449	−0.0193
0.97	−0.0161	0.0300	−0.0246	0.0026	−0.0411	−0.0170
0.98	−0.0144	0.0267	−0.0212	0.0027		

TABLE 9: Dimensions (angstroms) of the Box Modeling NBD[a]

d_x[b]	d_y[b]	d_z
6.5	6.5	5.4

[a] The van der Waals radii values are taken from ref 23. [b] Due to the symmetry of NBD, $d_x = d_y$ has been assumed, where d_x is the average of NBDs dimensions along the *x*- and *y*-axes.

5.2. On the Ordering of NBD in the Nematic Solutions. 5.2.1. Experimental Order Parameters. Once the adoption of eq 6 had been chosen, by making use of (B3LYP/6-31++G**)-calculated geometries and taking into account harmonic vibrational corrections (calculated by the B3LYP/6-31++G** force field with experimental IR frequencies; see the section above), we determined the "equilibrium" experimental ordering of NBD. The choice of molecular frame (shown in Figure 1) coinciding with the **S** matrix PAS, allowed us to work in a system where just two independent nonzero Saupe's parameters (or, equivalently, two independent linear combinations of them, as S_{zz} and $S_{xx} - S_{yy}$) were required to fully describe the orientational order of NBD: the values for different temperatures are reported in Table 8 (as a matter of fact, to investigate the existence of possible strong effects of the choice of geometries on order parameters, the same calculations have been repeated using different sets of geometries, different FFs, and using experimental and calculated vibrational frequencies. As shown in Figures SI-1 and SI-2 of the Supporting Information, only a small "scattering" in the **S** values has been observed; therefore, in the following discussion, the values of Table 8 will be always used).

Once the experimental order parameters of the solute at different temperatures in different solvents had been obtained, we started the phase of rationalization of NBD ordering in light of the application of the model proposed by Celebre [19,20] (and described above, in the Theoretical Section). The model allowed us to predict the solute orientation to be compared with experimental ordering data.

5.2.2. Calculation of Order Parameters by Numerical Simulations. MC simulations have been run to evaluate the total orientational solute−solvent interaction energy and thereafter determine the order parameters of the solute. In Table 9, the dimensions of the box describing the solute are given.

TABLE 10: Elements of the Electric Quadrupole Moment Tensor

Gaussian 98	Q_{xx}/ 10^{-40} C m^2	Q_{yy}/ 10^{-40} C m^2	Q_{zz}/ 10^{-40} C m^2
B3LYP/6-31++G**	−5.6	12.2	−6.6
LSDA/6-31++G**	−5.5	12.2	−6.7
RHF/6-31++G	−5.9	13.3	−7.4
RHF/6-31G**	−3.3	10.8	−7.6
experimental[a]	−5.3	11.2	−5.8
SCF/Aug-cc-pVDZ[a]	−6.2	13.7	−7.5

[a] From ref 24.

TABLE 11: Values of ϵ (Å^{-1} units) and F_{ZZ} (10^{17} V m^{-2} units) Used for MC Numerical Simulations

	EBBA		MM[a]	ZLI 1132	
T_{red}	ϵ	F_{ZZ}	ϵ	ϵ	F_{ZZ}
0.90				3.25	7.5
0.91	2.00	−9.0		3.00	7.0
0.92			2.00		
0.93				2.75	6.5
0.94	1.75	−8.5	1.75	2.5	6.0
0.95					
0.96			1.5	2.25	5.5
0.97	1.5	−8.0		2.00	5.0
0.98			1.25		
0.99	1.25	−7.5			

[a] F_{ZZ} (MM) = 0 assumed (see text for more explanations).

About the solute electric quadrupole tensor, several calculations were made by the GAUSSIAN 03 package,[38] using different methods and basis functions (see Table 10).

Since high-level calculated and experimental values resulted quite close, the use of experimental values was preferred (a short, general consideration can be made *en passant*: if experimental values of the molecular electric quadrupole tensor are not available, then calculations seem to be reliable when carried out by using DFT methods and extended basis functions). In Table 11, the values of ϵ and F_{ZZ}, chosen (by "trial and error") to perform the simulations, are given. The variation of reduced temperature is simulated by varying the value of ϵ, the parameter giving the strength of the solute−solvent short-range interaction; moreover, according to the "magic" nature of MM (vanishing of long-range orientational mechanisms), the EFG F_{ZZ}(MM) has been zeroed.

The MC numerical simulations were performed by using a homemade simulation program (see refs 19−22 for more details) running on an IBM intellistation 2.4 GHz (Linux O. S.). About 90 min were required for each run, where 10 000 configurations of the local solvent environment surrounding the box were randomly sampled for each of the 100 000 random global solute−solvent couple configuration generated. Experimental and MC-simulated order parameters of NBD in the three solvents are shown in Figure 5 (each of the simulated points in the figure is the average value obtained from a cycle of five runs); the corresponding numerical values, with standard deviations (±1% on experimental data, ±5% on simulated points), are reported in Table SI-5 of the Supporting Information (the statistical "uncertainties" of 5% attributed to the simulated data are to be ascribed to possible statistical fluctuations deriving from the necessarily finite number of configurations randomly sampled during the simulations: for more information, see ref 19 where this point is treated in detail).

5.2.3. Comparison between Experimental and Simulated Order Parameters. In the MM, as expected, the $U_{sr}(\beta,\gamma)$ short-range orientational interaction term (F_{ZZ} = 0 V m^{-2}) is enough to simulate successfully the complete orientational behavior of

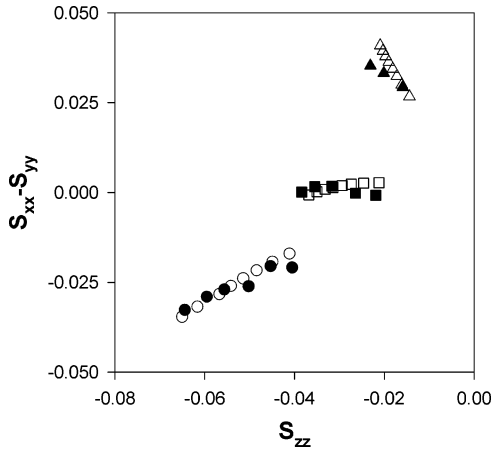

Figure 5. Experimental (open symbols) and simulated (full symbols) NBD order parameters in EBBA (triangles), MM (squares), and ZLI1132 (circles).

NBD. On the contrary, for a given value of T_{red} (i.e., for a fixed value of ϵ), the orientational ordering in the ZLI 1132 and EBBA phases are well reproduced by addition of the long-range potential term $U_{lr}(\beta,\gamma)$, with different-in-magnitude and opposite-in-sign values of F_{ZZ} (Table 11). Note that the short- and long-range terms are very well decoupled for NBD in EBBA, where, for a fixed T_{red} (see, for example, T_{red} = 0.94), the optimal ϵ value needed to gauge the short-range "ingredient" almost exactly matches the corresponding ϵ value in MM (at the same T_{red}); so, the "pure" addition of the proper long-range "ingredient" is enough to fully account for the ordering at that reduced temperature. On the contrary, for ZLI1132, both ϵ and F_{ZZ} must be modulated to reproduce effectively the ordering at that reduced temperature: this, in our opinion, is a "symptom" that, in this case, the quite crude assumption of simple additivity of short- and long-range orientational effects is not so good. A couple other interesting considerations can be made about the overall orientational results: (1) the fact that (for each phase) for a given variation of reduced temperature ΔT_{red} the same relative $-\Delta\epsilon$ (of course, opposite in sign) is found reflects that our simulation, although quite crude, is able to "capture" the essence of the physics of the orientational phenomenon (in other words, the ϵ values are not "randomly distributed" but, quite reasonably, they "scale" with reduced temperatures); (2) it is well-known that the "mean-field" approach is an approximation: actually, all real properties are influenced both by the solute and by the solvent, and ascribing a certain value of a property just to the solvent (independently from the solute) is an idealization. Anyway, the values of F_{ZZ} we found in this study for ZLI 1132 and EBBA are very similar to those given in Table 2 of ref 22 for the solute 1,4-difluorobenzene and to those obtained by other studies[25] (carried out using different approaches) for other various *p*-disubstituted benzenes in the same solvents at room temperature. Since the nature of our solute (NBD) is very different from *p*-disubstituted benzenes, this fact could suggest a certain possibility of transferability of the F_{ZZ} mean-field property. On the other hand, in this case, it should be explained why the F_{ZZ} values found for *p*-benzoquinone in the same mesophases (Table 2 of ref 22) are so different; so, also the possibility of a mere coincidence cannot be excluded in principle.

6. Conclusions

In our opinion, this work presents two main aspects of interest. The first concerns the controversial issue of possible

effects induced by the nematic solvents on the structure of the solute. In the present case, with the help of a DFT (B3LYP) calculation of vibrational corrections, we demonstrated that our data agree with a solution where the LXNMR-determined structure of NBD is compatible (within, at most, a 5% error) with the geometry predicted by high-level theoretical calculations. The small error found can be justified (at least partially) by taking into account the "physiological" consequences of the assumptions and approximations adopted in the treatment. The second significant achievement concerns the successful application of a recent model[19−22] to describe short- and long-range orientational interactions acting on small rigid molecules. The model, although very simple, proved to be very effective in predicting the basic mechanisms of ordering and useful in allowing conjectures and speculations about the complex nature of finer orientational effects.

Acknowledgment. This work has been financially supported by the Italian "Ministero dell'Istruzione, dell'Università e della Ricerca" (PRIN, "Modellizzazione e Caratterizzazione di Cristalli Liquidi per Strutture Nanorganizzate") and partially by the French "Ministère des Affaires Etrangères" (Lavoisier Fellowship).

Supporting Information Available: Additional tables about tested NBDs geometries (Table SI-1), vibrationally corrected dipolar couplings at different temperatures in EBBA (Table SI-2), MM (Table SI-3), and ZLI1132 (Table SI-4), and experimental and MC-calculated order parameters (Table SI-5). Additional figures about **S** dependence on the chosen geometry (Figure SI-1) and on the used frequencies (calculated or experimental) in vibrational corrections (Figure SI-2). This material is available free of charge via the Internet at http://pubs.acs.org.

References and Notes

(1) Emsley, J. W., Lindon, J. C., Eds. In *NMR Spectroscopy Using Liquid Crystal Solvents*; Pergamon: Oxford, U.K., 1975.

(2) Burnell, E. E., de Lange, C. A., Eds. In *NMR of Ordered Liquids*; Kluwer: Dordrecht, The Netherlands, 2003.

(3) Celebre, G.; De Luca, G.; Longeri, M. *Phys. Chem. Chem. Phys.* **2000**, *2*, 1883.

(4) Burnell, E. E.; de Lange, C. A. *Chem. Rev.* **1998**, *98*, 2359 and references therein.

(5) Vogel, A. I. *Vogel's Textbook of Practical Organic Chemistry*, 5th ed.; Longman: New York, 1989. March, J. *Advanced Organic Chemistry*, 4th ed.; Wiley: New York, 1992.

(6) (a) Lounila, J.; Jokisaari, J. *Prog. Nucl. Magn. Reson. Spectrosc.* **1982**, *15*, 249. (b) Vaara, J.; Jokisaari, J.; Wasylishen, R. E.; Bryce, D. L. *Prog. Nucl. Magn. Reson. Spectrosc.* **2002**, *41*, 233.

(7) Celebre, G.; De Luca, G.; Longeri, M.; Sicilia, E. *J. Chem. Inf. Comput. Sci.* **1994**, *34*, 539.

(8) Burnell, E. E.; Diehl, P. *Can. J. Chem.* **1972**, *50*, 3566.

(9) Sýkora, S.; Vogt, J.; Bösiger, H.; Diehl, P. *J. Magn. Reson.* **1979**, *36*, 53.

(10) Emsley, J. W.; Luckhurst, G. R. *Mol. Phys.* **1980**, *41*, 19.

(11) (a) Snijders, J. G.; de Lange, C. A.; Burnell, E. E. *J. Chem. Phys.* **1982**, *76*, 3474. (b) Burnell, E. E.; de Lange, C. A.; Mouritsen, O. G. *J. Magn. Reson.* **1982**, *50*, 188. (c) Snijders, J. G.; de Lange, C. A.; Burnell, E. E. *J. Chem. Phys.* **1982**, *77*, 5386. (d) Snijders, J. G.; de Lange, C. A.; Burnell, E. E. *J. Chem. Phys.* **1983**, *79*, 2964. (e) Burnell, E. E.; de Lange, C. A. *J. Magn. Reson.* **1980**, *39*, 461. (f) Lounila, J.; Diehl, P. *Mol. Phys.* **1984**, *52*, 827. (g) Lounila, J.; Diehl, P. *J. Magn. Reson.* **1984**, *56*, 254. (h) Lounila, J. *Mol. Phys.* **1986**, *58*, 897. (i) de Lange, C. A.; Snijders, J. G.; Burnell, E. E. In *Nuclear Magnetic Resonance of Liquid Crystals*; Emsley, J. W., Ed.; Reidel: Dordrecht, The Netherlands, 1985; p 181 and references therein. (j) Burnell, E. E.; de Lange, C. A.; Barnhoorn, J. B. S.; Aben, I.; Levelt, P. F. *J. Phys. Chem. A* **2005**, *109*, 11027.

(12) Shahkhatuni, A. A. *J. Mol. Struct.* **2005**, *743*, 217.

(13) Vaara, J.; Kaski, J.; Jokisaari, J. *J. Phys. Chem. A* **1999**, *103*, 5675.

(14) (a) Diehl, P. In *Encyclopedia of NMR*; Grant, D. M., Harris, M. K., Eds.; Wiley: New York, 1996; p 4591 and references therein. (b) De Luca, G.; Longeri, M.; Pileio, G.; Lantto, P. *ChemPhysChem* **2005**, *6*, 2086.

(15) Diehl, P. In *Nuclear Magnetic Resonance of Liquid Crystals*; Emsley, J. W., Ed.; Reidel: Dordrecht, The Netherlands, 1985; p 147 and references therein.

(16) Celebre, G.; De Luca, G.; Longeri, M.; Pileio, G.; Emsley, J. W. *J. Chem. Phys.* **2004**, *120*, 7075.

(17) Celebre, G.; Concistrè, M.; De Luca, G.; Longeri, M.; Pileio, G. *Chem.−Eur. J.* **2005**, *11*, 3599.

(18) Concistrè, M.; De Luca, G.; Longeri, M.; Pileio, G.; Emsley, J. W. *ChemPhysChem* **2005**, *6*, 1483.

(19) Celebre, G. *Chem. Phys. Lett.* **2001**, *342*, 375.

(20) Celebre, G. *J. Chem. Phys.* **2001**, *115*, 9552.

(21) Celebre, G.; De Luca, G. *J. Phys. Chem. B* **2003**, *107*, 3243.

(22) Celebre, G.; De Luca, G. *Chem. Phys. Lett.* **2003**, *368*, 359.

(23) Bondi, A. *J. Phys. Chem.* **1964**, *68*, 441.

(24) (a) Vogues, K.; Sutter, D. H.; Ruud, K.; Helgaker, T. *Z. Naturforsch., A: Phys. Sci.* **1998**, *53*, 67. (b) Vogelsanger, B.; Bauder, A. *J. Mol. Spectrosc.* **1988**, *130*, 249.

(25) (a) Syvitski, R. T.; Burnell, E. E. *J. Chem. Phys.* **2000**, *113*, 3452. (b) Dingemans, T.; Photinos, D. J.; Samulski, E. T.; Terzis, A. F.; Wutz, C. *J. Chem. Phys.* **2003**, *118*, 7046.

(26) Jensen, J. O. *J. Mol. Struct. (THEOCHEM)* **2005**, *715*, 7 and references therein.

(27) Wang, F.; Brunger, M. J.; Winkler, D. A. *J. Phys. Chem. Solids* **2004**, *65*, 2041 and references therein

(28) Brunelli, M.; Fitch, A. N.; Jouannaux, A.; Mora, A. J. *Z. Kristallogr.* **2001**, *216*, 51.

(29) Benet-Buchholz, J.; Haumann, T.; Boese, R. *J. Chem. Soc. Chem. Commun.* **1998**, 2003.

(30) Yokozeki, A.; Kuchitsu, K. *Bull. Chem. Soc. Jpn.* **1971**, *44*, 2356.

(31) Chiang, J. F.; Wilcox, C. F., Jr.; Bauer, S. H. *J. Mol. Struct. (THEOCHEM)* **1987**, *165*, 241.

(32) Knuchel, G.; Grassi, G.; Vogelsanger, B.; Bauder, A. *J. Am. Chem. Soc.* **1993**, *115*, 10845.

(33) Emsley, J. W.; Lindon, J. C. *Mol. Phys.* **1975**, *29*, 531.

(34) Cole, K. C.; Gilson, D. F. R. *J. Mol. Struct.* **1982**, *82*, 71.

(35) Syvitski, R. T.; Burnell, E. E. *J. Magn. Reson.* **2000**, *144*, 58.

(36) Granadino-Roldán, J. M.; Fernández-Gómez, M.; Navarro, A. *Chem. Phys. Lett.* **2003**, *372*, 255.

(37) Pileio, G. Ph.D. Thesis, Università della Calabria, Rende, Italy, 2005.

(38) Frisch, M. J.; Trucks, G. W.; Schlegel, H. B.; Scuseria, G. E.; Robb, M. A.; Cheeseman, J. R.; Montgomery, J. A., Jr.; Vreven, T.; Kudin, K. N.; Burant, J. C.; Millam, J. M.; Iyengar, S. S.; Tomasi, J.; Barone, V.; Mennucci, B.; Cossi, M.; Scalmani, G.; Rega, N.; Petersson, G. A.; Nakatsuji, H.; Hada, M.; Ehara, M.; Toyota, K.; Fukuda, R.; Hasegawa, J.; Ishida, M.; Nakajima, T.; Honda, Y.; Kitao, O.; Nakai, H.; Klene, M.; Li, X.; Knox, J. E.; Hratchian, H. P.; Cross, J. B.; Bakken, V.; Adamo, C.; Jaramillo, J.; Gomperts, R.; Stratmann, R. E.; Yazyev, O.; Austin, A. J.; Cammi, R.; Pomelli, C.; Ochterski, J. W.; Ayala, P. Y.; Morokuma, K.; Voth, G. A.; Salvador, P.; Dannenberg, J. J.; Zakrzewski, V. G.; Dapprich, S.; Daniels, A. D.; Strain, M. C.; Farkas, O.; Malick, D. K.; Rabuck, A. D.; Raghavachari, K.; Foresman, J. B.; Ortiz, J. V.; Cui, Q.; Baboul, A. G.; Clifford, S.; Cioslowski, J.; Stefanov, B. B.; Liu, G.; Liashenko, A.; Piskorz, P.; Komaromi, I.; Martin, R. L.; Fox, D. J.; Keith, T.; Al-Laham, M. A.; Peng, C. Y.; Nanayakkara, A.; Challacombe, M.; Gill, P. M. W.; Johnson, B.; Chen, W.; Wong, M. W.; Gonzalez, C.; Pople, J. A. *Gaussian 03*: Gaussian Inc.: Pittsburgh, PA, 2003.

(39) Park, G. H. J.; Martin, R. W.; Sakellariou, D.; Pines, A.; Shahkhatuni, A. G.; Shahkhatuni, A. A.; Panosyan, H. A. *Chem. Phys. Lett.* **2004**, *399*, 196.